

## In Situ Synthesis of Oligonucleotide Arrays by Using Surface Tension

John H. Butler,<sup>\*,†</sup> Maureen Cronin,<sup>‡</sup> Keith M. Anderson,<sup>§</sup> Giles M. Biddison,<sup>§</sup> Francois Chatelain,<sup>§</sup> Michael Cummer,<sup>§</sup> Deborah J. Davi,<sup>§</sup> Lawson Fisher,<sup>§</sup> Albrecht W. Frauendorf,<sup>§</sup> Felix W. Frueh,<sup>#</sup> Carmen Gjerstad,<sup>§</sup> Theresa F. Harper,<sup>||</sup> Stephanie D. Kernahan,<sup>§</sup> Danny Q. Long,<sup>§</sup> Mylan Pho,<sup>‡</sup> John A. Walker, II,<sup>⊥</sup> and Thomas M. Brennan<sup>§</sup>

Contribution from GenePharm Inc., 136 South Wolfe Road, Sunnyvale, California 94086, Aclara Biosciences, California, Protogene Laboratories, Inc., Menlo Park, California 94025, Lumicyte, Inc., California, Zyomyx, Inc., California, and Georgetown University Medical Center, Washington, DC 20007

Received October 23, 2000

**Abstract:** This work describes the in situ synthesis of oligonucleotide arrays on glass surfaces. These arrays are composed of features defined and separated by differential surface tension (surface tension arrays). Specifically, photolithographic methods were used to create a series of spatially addressable, circular features containing an amino-terminated organosilane coupled to the glass through a siloxane linkage. Each feature is bounded by a perfluorosilanated surface. The differences in surface energies between the features and surrounding zones allow for chemical reactions to be readily localized within a defined site. The aminosilanation process was analyzed using contact angle, X-ray photoelectron spectroscopy (XPS), and time-of-flight/secondary ion mass spectroscopy (TOF-SIMS). The efficiency of phosphoramidite-based oligonucleotide synthesis on these surface tension arrays was measured by two methods. One method, termed step-yields-by-hybridization, indicates an average synthesis efficiency for all four (A,G,C,T) bases of  $99.9 \pm 1.1\%$ . Step yields measured for the individual amidite bases showed efficiencies of 98.8% (dT), 98.0% (dA), 97.0% (dC), and 97.6% (dG). The second method for determining the amidite coupling efficiencies was by capillary electrophoresis (CE) analysis. Homopolymers of dT (40- and 60mer), dA (40mer), and dC (40mer) were synthesized on an NH<sub>4</sub>OH labile linkage. After cleavage, the products were analyzed by CE. Synthesis efficiencies were calculated by comparison of the full-length product peak with the failure peaks. The calculated coupling efficiencies were 98.8% (dT), 96.8% (dA), and 96.7% (dC).

## Introduction

Recently full or entire genomic sequences have been reported for several species. These include, among others, *Caenorhabditis elegans*,<sup>1</sup> *Saccharomyces cerevisiae*,<sup>2</sup> *Drosophila melanogaster*,<sup>3</sup> *Homo sapiens*,<sup>4</sup> and many others (<http://www.tigr.org/>). As a result, new technologies that are specifically designed for highly parallel analysis of the individual genes are emerging. Several private,<sup>5–14</sup> government,<sup>15</sup> and academic<sup>13,16–26</sup> institutions have developed analytical techniques based on the principal of

hybridizing labeled nucleic acid molecules to complimentary surface-tethered nucleic acid molecules (probes) as Southern proposed 25 years ago.<sup>27</sup>

<sup>†</sup> To whom correspondence should be addressed at GenoSpectra, Inc. 46540 Fremont Blvd., #506, Fremont, CA 94538. Telephone: 1-510-656-6500. Fax: 1-510-656-7200. E-mail: jbutler@genospectra.com.

<sup>‡</sup> Aclara Biosciences, Mountain View, CA 94043.

<sup>§</sup> Protogene Laboratories, Inc., Menlo Park, CA 94025.

<sup>⊥</sup> Lumicyte, Inc., Fremont, CA 94538.

<sup>||</sup> Zyomyx, Inc., Hayward, CA 94545.

<sup>#</sup> Georgetown University Medical Center, Washington, DC 20007.

(1) The *C. elegans* Sequencing Consortium. In *Science* **1998**, 282, 2012–2021.

(2) Goffeau, A.; Barrell, B. G.; Bussey, H.; Davis, R. W.; Dujon, B.; Feldmann, H.; Galibert, F.; Hoheisel, J. D.; Jacq, C.; Johnston, M.; Louis, E. J.; Mewes, H. W.; Murakami, Y.; Philippsen, P.; Tettelin, H.; Oliver, S. G. *Science* **1996**, 274, 546, 563–567.

(3) Adams, M. D.; Celniker, S. E.; Holt, R. A.; Evans, C. A.; Gocayne, J. D.; et al. *Science* **2000**, 287, 2185–2195.

(4) (a) The International Human Genome Sequencing Consortium. In *Nature* **2001**, 409, 860–921. (b) Venter, J. C.; Adams, M. D.; Myers, E. W.; Li, P. W.; Mural, R. J.; et al. *Science* **2001**, 291, 1304–1351.

(5) Saizieu, A.; Certa, U.; Warrington, J.; Gray, C.; Keck, W.; Mous, J. *Nat. Biotechnol.* **1998**, 16, 45–48.

(6) Wallraff, G.; Nguyen, T.; Labadie, J.; Huynh, T.; Brock, P.; Hinsberg, W.; DiPietro, R.; McGall, G. *Chemtech* **1997**, 22–32.

(7) McGall, G.; Labadie, J.; Brock, P.; Wallraff, G.; Nguyen, T.; Hinsberg, W. *Proc. Natl. Acad. Sci. U.S.A.* **1996**, 93, 13555–13560.

(8) Pease, A.; Solas, D.; Sullivan, E. J.; Cronin, M. T.; Holmes, C. P.; Fodor, S. P. A. *Proc. Natl. Acad. Sci. U.S.A.* **1994**, 91, 5022–5026.

(9) Chee, M.; Yang, R.; Hubbell, E.; Berno, A.; Huang, X. C.; Stern, D.; Winkler, J.; Lockhart, D. J.; Morris, M. S.; Fodor, S. P. A. *Science* **1996**, 274, 610–614.

(10) Lockhart, D.; Dong, H.; Byrne, M. C.; Follett, M. T.; Gallo, M. V.; Chee, M. S.; Mittmann, M.; Wang, C.; Kobayashi, M.; Horton, H.; Brown, E. L. *Nat. Biotechnol.* **1996**, 14, 1675–1680.

(11) Lamture, J.; Beattie, K. L.; Burke, B. E.; Eggers, M. D.; Ehrlich, D. J.; Fowler, R.; Hollis, M. A.; Kosicki, B. B.; Reich, R. K.; Smith, S. R.; Varma, R. S.; Hogan, M. E. *Nucleic Acids Res.* **1994**, 22, 2121–2125.

(12) Little, D.; Cornish, T. J.; O'Donnell, M. J.; Braun, A.; Cotter, R. J.; Koster, H. *Anal. Chem.* **1997**, 69, 4540–4546.

(13) Schena, M.; Heller, R. A.; Theriault, T. P.; Konrad, K.; Lachenmeier, E.; Davis, R. W. *Trends Biotechnol.* **1998**, 16, 301–306.

(14) Brennan, T. M. U.S. Patent number 5474796, December 12, 1995.

(15) (a) Chrisey, L. A.; Lee, G. U.; O'Ferrall, C. E. *Nucleic Acids Res.* **1996**, 24, 3031–3039. (b) Chrisey, L.; O'Ferrall, C. E.; Spargo, B. J.; Dulcey, C. S.; Calvert, J. M. *Nucleic Acids Res.* **1996**, 24, 3040–3047.

(16) Schena, M.; Shalon, D.; Davis, R. W.; Brown, P. O. *Science* **1995**, 270, 467–470.

(17) Schena, M.; Shalon, D.; Heller, R.; Chai, A.; Brown, P. O.; Davis, R. W. *Proc. Natl. Acad. Sci. U.S.A.* **1996**, 93, 10614–10619.

(18) Guo, Z.; Guilfoyle, R. A.; Thiel, A. J.; Wang, R.; Smith, L. M. *Nucleic Acids Res.* **1994**, 22, 5456–5465.

(19) Case-Green, S.; Mir, K. U.; Pritchard, C. E.; Southern, E. M. *Curr. Opin. Chem. Biol.* **1998**, 2, 404–410.

(20) Shechinov, M.; Case-Green, S. C.; Southern, E. M. *Nucleic Acids Res.* **1997**, 25, 1155–1162.

Methods of producing these hybridization arrays include coupling (via contact printing or spotting) synthetic oligonucleotides to surfaces,<sup>15,18,29</sup> adsorbing cDNA on to positively charged surfaces,<sup>13,16,17</sup> and in situ synthesis of probes directly on a surface using either photolithographic, physical masking, or ink-jet printing approaches.<sup>5–11,15,18–22,28,50</sup> All of these methods have been shown to generate arrays that yield a great deal of information and are useful for particular applications. However, each technology also has significant limitations in its application or availability. cDNA arrays depend on the availability of clone libraries that are of limited availability and may be in low supply. However, recent programs have pooled cloning efforts to produce cDNA microarrays that will eventually contain the entire expressed human genome.<sup>30</sup> Another concern is that the amount of cDNA or synthetic oligonucleotide material deposited by spotting may vary from feature to feature on an array thus limiting quantitative comparisons between features in one-color assays. However, this limitation is overcome in two-color ratio determinations within individual features.

Covalent coupling of presynthesized oligonucleotides on to array surfaces<sup>29</sup> offers some advantages including the purification and analytical characterization of the probes prior to attachment to the surface. However, wide flexibility in array probe design is still limited by the high cost of presynthesizing large oligonucleotide libraries prior to spotting. In situ synthesis of probes presents other limitations. The most recognized technology employs phosphoramidites with photolabile protecting groups together with a photolithographic masking procedure to direct amidite coupling to specific regions on a glass surface.<sup>7,8,31</sup> In this process, base coupling is controlled by two reactions, deprotection of the 5' hydroxyl with subsequent coupling of the 3' phosphoramidite to the deprotected 5' hydroxyl. While the coupling via the phosphoramidite chemistry is efficient, incomplete removal of the MeNPOC<sup>31a</sup> protecting group on the 5' hydroxyl would lead to a percentage of protected bases that are not accessible to coupling of the next base and if removed in a subsequent round of deprotection would lead to a percentage of deletion sequences within any given feature. If present, these internal deletions<sup>31</sup> would affect the quality of the synthesis, and therefore would affect the overall hybridization signal. As a result of any incomplete deprotection, the resulting per-base coupling efficiency of the light-directed deprotection reaction chemistry may be limited with respect to the length of the probe that can be synthesized. With the best reported stepwise coupling efficiencies of 92 to 94%,<sup>31a</sup> the amount of full length product in any given feature is maximally

12 to 21% (assuming a 25mer oligonucleotide), but improvements to light-directed deprotection and overall coupling yields have recently been reported,<sup>31b</sup> increasing the potential 25mer yield to greater than 77%. Even though the coupling yields do not match standard phosphoramidite chemistry yields, these substrates perform well in genomic studies.<sup>5,8–10,19,32</sup>

Two other methods of synthesizing oligonucleotide probes in situ on DNA chips use standard phosphoramidite chemistry and deprotection.<sup>20–22,50</sup> In one version,<sup>23</sup> reagents are introduced into a chamber that is pressed against the surface of a solid support to make a reagent flow cell. The reaction cell is moved along by a fraction of its diameter at each coupling step, resulting in a series of oligonucleotides of overlapping sequence laid out along the synthesis path. The length of the longest sequence made is equal to the diameter of the flow cell divided by the offset used at each coupling step. Even though the coupling efficiencies remain high, analysis is often limited to a single gene per chip due to the dimensional limitations of the flow cell and substrate. Another approach to fabricating arrays by in situ synthesis uses ink-jet delivery of phosphoramidites to microarrays and has demonstrated the synthesis of probes up to 60 bases in length with stepwise coupling efficiencies reported from 94 to 98%. These arrays have been utilized in gene expression studies although the details of the chemistry have not been discussed.<sup>50</sup>

Here we report an approach to preparing oligonucleotide arrays by in situ synthesis that uses standard nucleoside phosphoramidite chemistry and dimethoxytrityl-based protec-

(21) Maskos, U.; Southern, E. M. *Nucleic Acids Res.* **1992**, *20*, 1679–1684.

(22) Maskos, U.; Southern, E. M. *Nucleic Acids Res.* **1992**, *20*, 1675–1678.

(23) Southern, E. M. *Trends Genet.* **1996**, *12*, 110–113.

(24) Yershov, G.; Barsky, V.; Belgovskiy, A.; Kirillov, E.; Kreindlin, E.; Ivanov, I.; Parinov, S.; Guschin, D.; Drobishev, A.; Dubiley, S.; Mirzabekov, A. *Proc. Natl. Acad. Sci. U.S.A.* **1996**, *93*, 4913–4918.

(25) Parinov, S.; Barsky, V.; Yershov, G.; Kirillov, E.; Tomofeev, E.; Belgovskiy, A.; Mirzabekov, A. *Nucleic Acids Res.* **1996**, *24*, 2998–3004.

(26) Drobishev, A.; Mologina, N.; Shik, V.; Pobedinskaya, D.; Yershov, G.; Mirzabekov, A. *Gene* **1997**, *188*, 45–52.

(27) Southern, E. M. *J. Mol. Biol.* **1975**, *98*, 503–517.

(28) Fodor, S. P. A.; Leighton-Read, J.; Pirrung, M. C.; Stryer, L.; Lu, A. T.; Solas, D. *Science* **1991**, *251*, 767–773.

(29) Drmanac, S.; Kita, D.; Labat, I.; Hauser, B.; Burczak, J.; Dramanac, R. *Nat. Biotechnol.* **1998**, *16*, 54–58.

(30) Lennon, G.; Auffray, C.; Polymeropoulos, M.; Soares, M. B. *Genomics* **1996**, *33*, 151–152.

(31) (a) McGall, G.; Barone, A. D.; Diggelmann, M.; Fodor, S. P. A.; Gentalen, E.; Ngo, N. *J. Am. Chem. Soc.* **1997**, *119*, 5081–5090. (b) Beier, M.; Hoheisel, J. D. *Nucleic Acids Res.* **2000**, *28*, e11.

(32) (a) Cronin, M. T.; Fucini, R. V.; Kim, S. M.; Masino, R. S.; Wespi, R. M.; Miyada, C. G. *Hum. Mutat.* **1996**, *7*, 244–255. (b) Forman, J. E.; Walton, I. D.; Stern, D.; Rava, R. P.; Trulson, M. O. *ACS Symp. Ser.* **1998**, *682*, 206–228.

(33) (a) Beaucage, S. L.; Caruthers, M. H. *Tetrahedron Lett.* **1981**, *22*, 1859–1862. (b) Matteucci, M. D.; Caruthers, M. H. *J. Am. Chem. Soc.* **1981**, *103*, 3185–3191.

(34) Caruthers, M. H. *Acc. Chem. Res.* **1991**, *24*, 278–284.

(35) Beaucage, S. L.; Iyer, R. P. *Tetrahedron* **1992**, *48*, 2223–2311.

(36) Blanchard, A. P.; Kaiser, R. J.; Hood, L. E. *Biosens. Bioelectron.* **1996**, *11*, 687–690.

(37) Fadeev, A. Y.; McCarthy, T. J. *Langmuir* **1999**, *15*, 3759–3766.

(38) Matsuzawa, M.; Tokumitsu, S.; Knoll, W.; Sasabe, H. *Langmuir* **1998**, *14*, 5133–5138.

(39) (a) Lardon, B.; Kovats, E. *Adv. Colloid Interface Sci.* **1976**, *6*, 95–137. (b) Kirkland, J. J.; Glajch, J. L.; Farlee, R. D. *Anal. Chem.* **1989**, *61*, 2–11. (c) Hetem, M. J. J.; De Haan, J. W.; Claessens, H. A.; Cramers, C. A.; Degee, A.; Schomburg, G. *J. Chromatogr.* **1991**, *540*, 53–76.

(40) (a) Vandenberg, E.; Bertilsson, L.; Liedberg, B.; Uvdal, K.; Erlandsson, R.; Elwing, H.; Lundstrom, I. *J. Colloid Interface Sci.* **1991**, *147*, 103–119. (b) Blackledge, C.; McDonald, J. D. *Langmuir* **1999**, *15*, 8119–8125.

(41) Gray, D. E.; Case-Green, S. C.; Fell, T. S.; Dobson, P. J.; Southern, E. M. *Langmuir* **1997**, *13*, 2833–2842.

(42) Parikh, A. N.; Allara, D. L. *J. Phys. Chem.* **1994**, *98*, 7577–7590.

(43) Brzoska, J. B.; Ben Azouz, I.; Rondelez, F. *Langmuir* **1994**, *10*, 4367–4373.

(44) Brzoska, J. B.; Shahidzadeh, N.; Rondelez, F. *Nature* **1992**, *360*, 719–721.

(45) (a) Hozumi, A.; Ushiyama, K.; Sugimura, H.; Takai, O. *Langmuir* **1999**, *15*, 7600–7604. (b) Haller, I. *J. Am. Chem. Soc.* **1978**, *100*, 8050–8055.

(46) Heiney, P. A.; Grüneberg, K.; Fang, J.; Dulcey, C.; Shashidhar, R. *Langmuir* **2000**, *16*, 2651–2657.

(47) Takeda, Y.; Saga, M.; Ogawa, K.; Ozaki, S. *Polym. Prepr. Jpn.* **1993**, *42*, 1717.

(48) (a) SantaLucia, J., Jr. *Proc. Natl. Acad. Sci. U.S.A.* **1998**, *95*, 1460–1465. (b) Peyret, N.; Senevirante, P. A.; Allawi, H. T.; SantaLucia, J., Jr. *Biochemistry* **1999**, *38*, 3468–3477.

(49) Frueh, F. W.; Hon, S.-Y. C.; Flockhart, D. A.; Woosley, R. L. *Pharmacogenetics*. Submitted for publication.

(50) Hughes, T. R.; Mao, M.; Jones, A. R.; Burchard, J.; Marton, M. J.; Shannon, K. W.; Lefkowitz, S. M.; Ziman, M.; Schelter, J. M.; Meyer, M. R.; Kobayashi, S.; Davis, C.; Dai, H.; He, Y. D.; Stephaniants, S. B.; Cavet, G.; Walker, W. L.; West, A.; Coffey, E.; Shoemaker, D. D.; Stoughton, R.; Blanchard, A. P.; Friend, S. H.; Linsley, P. S. *Nat. Biotechnol.* **2001**, *19*, 342–347.

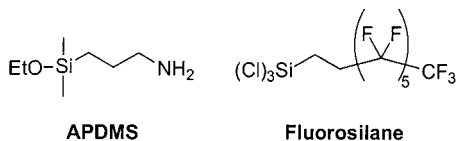


**Figure 1.** Silanes used for the creation of surface tension arrays.

tion.<sup>33–35</sup> This approach to array synthesis uses differential surface tension to define each synthesis site and produce what we term “surface tension arrays”.<sup>14,36</sup> By using a mixed solvent system (10% acetonitrile:90% adiponitrile) that limits evaporation during reagent delivery and during amidite coupling reactions, near quantitative coupling efficiencies are achieved using piezoelectric, ink-jet, reagent delivery of the nucleoside phosphoramidite monomers. Because these piezoelectric nozzles are computer-controlled ink jets, very fast, iterative design refinements may be incorporated into the assay (chip) development with little or no economic penalty. A simple process for the production of surface tension arrays is discussed. Determination of coupling efficiencies and oligonucleotide quality are measured by two different methods and the results are shown to be comparable to conventional solid-phase oligonucleotide synthesis products. One method is based on the hybridization of a complementary target to a mixed sequence probe that has been synthesized at the 5'-ends of sequentially increasing lengths of poly-dT, -dA, -dC, and -dG linkers. Confirming results were shown with CE data for the oligonucleotide product cleaved after 40 successive amidite couplings and synthesis step yields calculated from the failure product peaks in the electropherogram.

## Results and Discussion

Several performance criteria were established at the outset of developing this technology. The first requirement was to develop a surface preparation that would allow us to produce consistent, densely packed substrates for oligonucleotide synthesis and at the same time provide a hydrolytically stable linkage between the oligonucleotide probe and the glass surface. The process was developed using a monofunctional (one attachment site for silanation) organosilane, 3-aminopropyltrimethoxysilane (APDMS, **1**, Figure 1).<sup>37,38</sup> Trialkylsilanes have been shown to efficiently react with available surface silanols and pack to densities that render any remaining surface silanols essentially nonreactive.<sup>37,39</sup> The silane, due to its single hydrolyzable group, can only be covalently bonded to the glass substrate through a single siloxane bond. This eliminates the branched polymerizations that are possible using trifunctional silanes (three attachment sites for silanation) that can lead to variations in the density of reactive sites across an individual array. Due to the ordered packing, the hydrolytic stability of the monofunctional silane bond is preserved at low to moderate pH ranges<sup>39</sup> and any hydrogen bonding by the amine groups with the surface silanols is inhibited, thus allowing for all amines to be available for subsequent reactions.<sup>40</sup> In contrast, most array technologies use a trifunctional silane for the initial derivatization of the surface.<sup>7,8,41,42</sup> Solution-phase monolayer formation using trifunctional silanes is a process highly dependent upon a variety of parameters including time, temperature, solvent, water concentrations, catalysts, silane concentration, free silanol densities, and substrate status.<sup>40a</sup> Monolayer formation using trifunctional silanes is subject to strict control of the surface derivatization conditions and can lead to a percentage of multilayer polymer formation and a poor control over the surface density.<sup>42–44</sup> Vapor-phase silanation has been reported to work

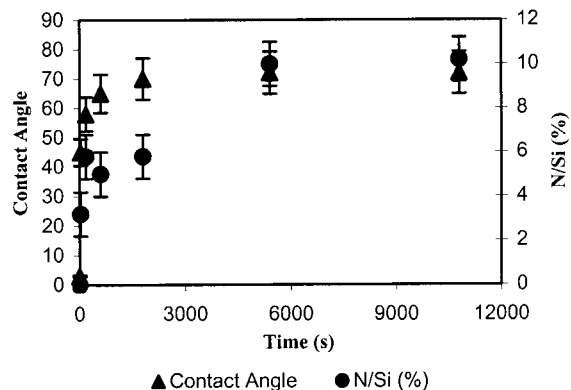


**Figure 2.** Plot of water contact angle (left Y-axis) and XPS-derived concentration of nitrogen atoms (right Y-axis) as a function of the aminosilanation reaction time.

well for monolayer formation with use of trifunctional silanes<sup>45</sup> and is currently under evaluation in these laboratories.

A second goal in derivatizing glass with APDMS was to achieve as complete a functionalization of the surface as possible with a robust, reproducible process. To achieve this aim, a prederivatization process that gave a uniformly clean substrate was required. This process included a detergent washing and water rinse of the glass substrates, followed by exposure to an oxygen plasma, treatment with Piranha solution, and then a second exposure to the oxygen plasma. XPS analysis of the surfaces prior to the initial silanation step indicated a surface free of contaminants outside of adventitious molecules and a water contact angle  $\leq 5^\circ$ . The aminosilanation reaction was characterized next. As can be seen in Figure 2, the water contact angle increased substantially during the first 30 min of silanation and, after 90 min, asymptotically approached  $72^\circ$ . Interestingly, when the contact angles were measured prior to curing at  $120^\circ\text{C}$  for 60 min, the same trend was observed, but the curve increased to the asymptote more gradually. XPS data also indicated that the APDMS density was increasing. Figure 2 shows that the apparent density of the APDMS layer increased with time for 90 min. After that the concentration of nitrogen atoms began to level off relative to the concentration of silicon atoms.

Time-of-flight secondary ion mass spectroscopy (TOF-SIMS) analysis of these aminosilated surfaces shows that, along with chemisorbed molecules, there are physisorbed impurities which can lead to aberrations in the XPS data and a lower N/Si ratio. If the glass surface is decorated with APDMS groups that are covalently attached to the surface through a siloxane linkage, then fragment ions such as  $\text{SiNOC}_3\text{H}_{14}$ ,  $\text{SiNC}_3\text{H}_{14}$ ,  $\text{SiNOC}_4\text{H}_{11}$ ,  $\text{SiNOC}_3\text{H}_8$ , and  $\text{SiNC}_3\text{H}_8$  should be apparent in the mass spectrum. Indeed, these fragments are observed and support this conclusion, although they do not prove that the APDMS attaches covalently to the surface. Other fragments observed in the mass spectrum contain ions that can be attributed to bis[(aminopropyl)tetramethyldisiloxane] impurities that are present in the starting APDMS or result from noncovalent association of the ethoxysilane with the glass. We have found that vacuum curing the substrates following silanation removes a majority of these physisorbed materials and we have subsequently incorporated this into our process. Our observations are consistent with others who have shown that contact angle and XPS measurements follow the same trendlines.<sup>46</sup>

For the subsequent surface patterning, a positive photoresist was used to protect the intended synthesis features during application of a fluorophilic mask. Following photoresist



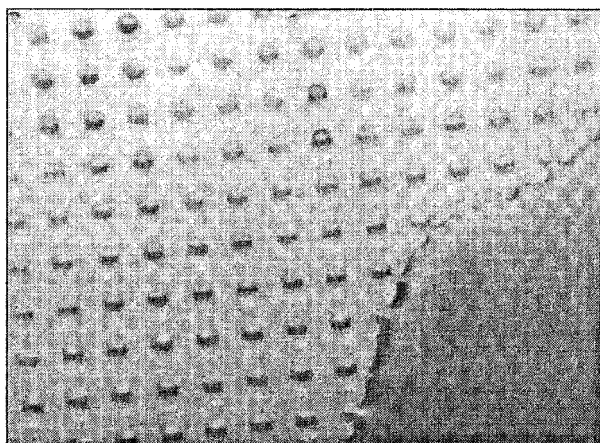


**Figure 3.** Photograph of a demonstration of the surface tension array's differential wetting phenomena. A patterned slide was immersed in water, removed, and tilted to allow the liquid to flow off of the surface. As can be seen, the hydrophilic aminosilated areas retain the liquid within the feature while the fluorophilic mask area allows the water to sheath off the surface.

exposure and development, an oxygen plasma treatment removed any exposed amine groups and resulted in a "clean" glass surface that was then treated with (tridecafluoro-1,1,2,2-tetrahydrooctyl)trichlorosilane (**2**), perfluorosilane. The resulting "fluorophilic" region has similar material properties of Teflon. The perfluorosilane used to create this surface is only solubilized, or "wetted", by other fluorocarbon substances; it is not wetted by other solvents. Therefore, the oligonucleotide synthetic chemistries are only localized within the aminosilated features. The fluorophilic region consistently had water contact angles on the order of  $105^\circ \pm 2^\circ$  and was within the reported values for glass surfaces functionalized with **2**.<sup>47</sup> The wetting characteristics of the resulting surface tension arrays are depicted in Figure 3. A glass substrate was prepared as described (vide supra) and then submerged in water. Upon removal from the water with a slight tilting of the substrate, one can see that the difference in surface tension "holds" water within the hydrophilic features. This differential wetting phenomenon also occurs with polar organic solvents and it is this property that constrains the subsequent synthetic chemistry reactions to those sites. Fluorescent measurements of features directly labeled with Cy3-dye as well as measurement of individual features with a light microscope have shown that the feature size variability is less than 4%.

The goal in developing this process was to make arrays that not only have a low variance in signal intensities within an array (intra-array), but are also reproducible from array to array (inter-array). To demonstrate the uniformity and reproducibility of array fabrication, we used fluorescence-based techniques. A succinimidyl-terminated Cy3 monofunctional dye was coupled to the surface-bound amines in intended synthesis sites. The data showed 11.5% intra-array and inter-array variations as measured by fluorescence intensity. This result was derived from analysis of 2511 features/array, using 10 individual arrays from 10 separate array batches. Similarly, 5' end-labeling of an in situ synthesized 20mer mixed sequence (3'-GAGTTCTACGATGGCAAGTC-5', **C20**) with Cy3 phosphoramidite allowed us to determine the variance in signal after 20 coupling cycles. In this case, following in situ oligonucleotide synthesis, end labeling, and deprotection, we observed a 12% inter-array variation in full-length product signal. These results show that the process we have developed for synthesis is reproducible over multiple batches.

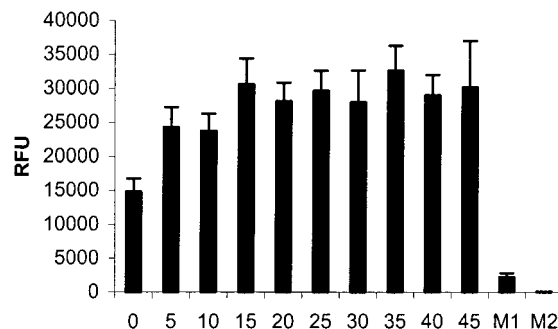


**Figure 4.** Step yield by hybridization. Relative fluorescence values (RFU) were generated by using the GenePix analysis program on the Axon Instruments GenePix4000A scanner after hybridization of the arrays as described in the text. An array of oligonucleotides made of varying lengths of a repeated mixed sequence, (AGTC)<sub>n</sub>, from 5 to 45 couplings were synthesized followed by a common 10mer (3'-GCCATCGTAG, **C10**). Also, after 45 coupling of the mixed sequence (AGTC)<sub>n</sub>, two 10mers (3'-GCCAgCGTAG, **M1**, and 3'-GCCAgaGTAG, **M2**) were synthesized on the same array that were single (**M1**) and double (**M2**) double base pair mismatches of the **C10** sequence. The sequences synthesized at each probe were as follows: **0** = **C10**, **5** = 3'-(AGTC)A-C**10**, **10** = 3'-(AGTC)<sub>2</sub>AG-C**10**, **15** = 3'-(AGTC)<sub>3</sub>AGT-C**10**, **20** = 3'-(AGTC)<sub>5</sub>-C**10**, **25** = 3'-(AGTC)<sub>6</sub>A-C**10**, **30** = 3'-(AGTC)<sub>7</sub>AG-C**10**, **35** = 3'-(AGTC)<sub>8</sub>AGT-C**10**, **40** = 3'-(AGTC)<sub>10</sub>-C**10**, **45** = 3'-(AGTC)<sub>11</sub>A-C**10**, **M1** = 3'-(AGTC)<sub>11</sub>A-M**1**, **M2** = 3'-(AGTC)<sub>11</sub>A-M**2**.

The direct labeling experiments gave an indication of the uniformity of the core chemistry of the arrays, but do not necessarily predict functional assay performance. To address the uniformity of the arrays under functional conditions, we again surveyed multiple sites on arrays from 10 synthesis batches. Cy3 labeled 20mer compliments were allowed to hybridize to 258 different sites per array in 6XSSC (0.09 M sodium citrate, pH 7.0, 0.9 M sodium chloride) for 30 min at 22 °C. The arrays were washed for 5 min in fresh buffer and dried, and fluorescence intensities were measured using a GenePix4000A array scanner (Axon Instruments). The fluorescence variation among features and the signal variation within each feature (intra-feature) were measured. We found a 14% variation across an array and a 10% variance within features. These results indicate that the synthetic uniformity of the arrays as measured through indirect functional methods is consistent with direct measurements.

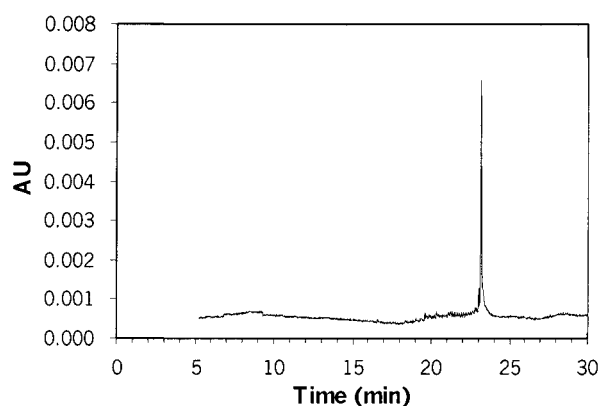
To calculate the average step yields of chemical reactions using piezoelectric drop-on-demand delivery of phosphoramidite solutions, an array of oligonucleotides made by varying the length of a repeated mixed sequence, (AGTC)<sub>n</sub>, was synthesized followed by a common 10mer (3'-GCCATCGTAG, designated **C10**). The **C10** sequence was complementary to the central 10 bases of the 20mer hybridization target, **C20**. After deprotection and washing, the oligonucleotide array was immersed in 30 mL of hybridization buffer, 6XSSC (0.09 M sodium citrate, pH 7.0, 0.9 M sodium chloride), containing 20 nM of 5'-Cy3 end-labeled **C20** for 30 min at 22 °C, washed for 5 min in fresh buffer, dried, and imaged with the GenePix4000A array scanner.

Figure 4 shows a plot of the fluorescence normalized to the length of the mixed sequence monomers. In all experiments, the fluorescence signal from the spots with the **C10** probe synthesized directly from the hexaethylene glycol-based linker (vide infra) was lower than the fluorescence signal from the features where the **C10** was synthesized on the AGTC repeats. This low signal may be due to a very high density of probe oligo resulting in steric inhibition of target access to the probe. Alternatively, local environmental phenomena may result in a

reduced quantum efficiency of the fluorophore.<sup>51</sup> Single base (3'-GCCAgCGTAG, designated **M1**) and double base (3'-GCCAgAGTAG, designated **M2**) mismatched hybridization control probes were included to measure the specificity of the hybridizable signal. Using the HyTher (<http://jsl1.chem.wayne.edu/Hyther/hythermenu.html>)<sup>48</sup> program for prediction of nucleic acid hybridization thermodynamics and the following parameters, 0.9 M NaCl, 20 nM target, and 22 °C,  $T_m$  values of 37.7, 26.6, and 8.2 °C for the perfect, single, and double mismatches, respectively, are predicted. In Figure 4 the fluorescence signal for **M1** and **M2** after 45 mixed sequence couplings was compared to the exact compliment signal. The hybridization signal for the single and double base mismatch probes was 7.3% and 0.2% of the exact match, respectively. This indicates that the hybridization signals for the complimentary features are specific and indicate high synthesis fidelity. The average step yield for mixed sequences was calculated by comparing the fluorescence signals in the features with the mixed sequence extensions and was found to be  $99.9 \pm 1.1\%$ . Finally, this technique was used to calculate the coupling efficiencies for the individual nucleotides through synthesis of **C10** to the 5'-ends of homopolymers of dT, dA, dC, and dG and the coupling efficiencies were 98.8, 98.0, 97.0, and 97.6%, respectively.

We also have calculated the density of synthesized probes and hybridization capacity using two fluorescence-based techniques. First, after establishing the linear range of relative fluorescence units (RFU) on the GenePix 4000A at a photomultiplier tube (PMT) setting of 400, we spotted known quantities of Cy3 labeled **C20** in water to three slides, dried the samples, and then imaged the slides in the green channel. The data derived from the experiments was averaged and plotted as RFU vs density of fluorophore ( $\text{mol}/\text{mm}^2$ ) and a linear curve fit gave an equation that related these two values. We found that the fluorescence values were linear with an  $R^2$  value of 0.993 up to densities of  $100 \text{ fmol}/\text{mm}^2$ . We then developed a second method for relating RFU and density of probe using a target depletion hybridization assay. This technique was developed to relate hybridizable fluorescence to absolute fluorescence as a measure of synthesis density. First, several arrays were produced that had the same sequence (3'-CAGTTGCATCGTAGAACTC, **C20comp**, complimentary to **C20**) synthesized in every feature. Then concentrations of 0.88 and 1.76 nM (0.88 and 1.76 pmol, respectively, in 1.0 mL of 6XSSC) of Cy3-labeled **C20** were allowed to hybridize to the arrays. The hybridization was allowed to go until such a time as there was no detectable absorption at 530 nm (peak absorption for Cy3) and 260 nm in the hybridization solution. After summing the total fluorescence across all features, we saw an increase in the fluorescence signal from 0.88 to 1.76 nM of 2.0-fold and the values were within the linear range of the first experiment. Comparison of the data sets from both experiments was accurate to within a variation of 10% in the calculated densities, suggesting that the approaches were a good approximation of the amount of fluorophore.

To determine the maximal hybridizable density, we hybridized to saturation by placing arrays that had **C20comp** synthesized in every feature into a solution containing Cy3 labeled **C20** (600 pmol in 30 mL of 6XSSC), scanned the slide, and rehybridized in a fresh solution until the amount of fluorescence did not increase. Using the equations derived from the standardization experiments, the data from this experiment gave an average density of hybridizable probe of  $21.4 \pm 4.2 \text{ fmol}/\text{mm}^2$ . The calculation of synthesized probe density was determined



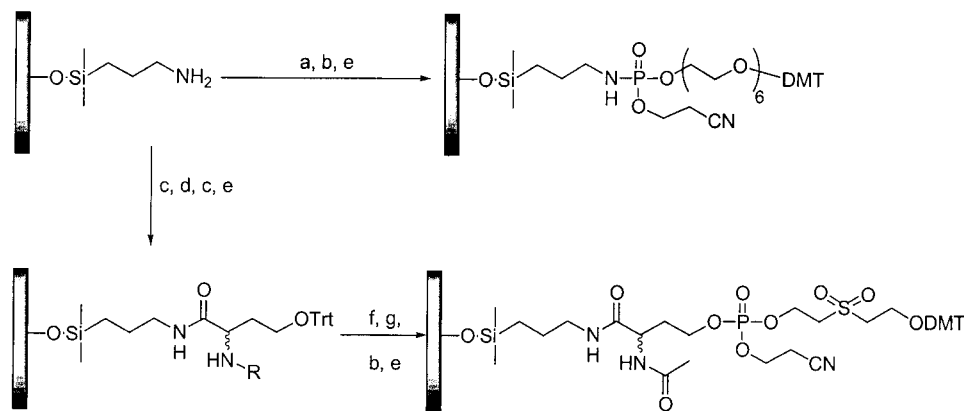
**Figure 5.** Capillary electrophoresis analysis of a  $\text{dC}_{40}$  prepared on a surface tension array. After 40 dC-amidite couplings, the synthesis product was released via use of a base-labile linker as described in the text.

after 5' end labeling of **C20comp** with Cy3 phosphoramidite and quantification of fluorescence using the same approach. We calculated a value of  $51.0 \pm 5 \text{ fmol}/\text{mm}^2$ , indicating that approximately 42% of the sites are available for hybridization to small labeled oligonucleotides. Because the calculated values were within the linear range of the standard curve, the values approximate the density without any potential influence due to fluorophore quenching. These values are in agreement with other reported values, independent of the oligonucleotide being spotted<sup>15a</sup> or prepared in situ.<sup>22,32b</sup>

A detailed discussion of buffer/array stability is outside the scope of this report, but some general comments may be made. As noted by others,<sup>22,41</sup> the use of the standard reagent for oligonucleotide deprotection, ammonium hydroxide, results in probe loss from the array surface. We also observed this effect and have found that using ethylenediamine/ethanol (EDA/EtOH; 1:1) for array deprotection does not result in loss of probe from the surface. Time-course studies for complete deprotection show a gradual increase in hybridization signal and then a leveling of hybridized fluorescence after 2 h for the fast-deprotecting (phenoxyacetyl-based, PAC) amidites, and treatment with the EDA/EtOH solution for up to 16 h at room temperature resulted in no loss of Cy3 end-labeled or hybridization-related fluorescence signal on the arrays. Also, buffers used for hybridization studies in this report were not seen to compromise the integrity of the array. A detailed study of array stability in various buffers is forthcoming; however, we have found that under the hybridization conditions presented here, the arrays are stable for at least 8 h.

To directly demonstrate the per-base coupling efficiency, 40mers were synthesized on 2-[2-(4,4'-dimethoxytrityloxy)-ethylsulfonyl]ethyl-(2-cyanoethyl)-(N,N-diisopropyl)-phosphoramidite (CPR-I) derivatized surfaces (Scheme 1), then cleaved and deprotected with aqueous ammonia. Figure 5 shows an electropherogram for  $\text{dC}_{40}$  prepared on our substrates. The step yield calculations were based on comparison of the failure peaks to the full-length product. As can be seen, the homopolymer was very pure. For the preparation of  $\text{dC}_{40}$ , the average step yield based upon integration of the failure peaks was 96.7%. We also calculated these numbers for  $\text{dT}_{40}$  (98.8%) and  $\text{dA}_{40}$  (96.8%). We were unable to synthesize and analyze a clean  $\text{dG}_{40}$  homopolymer, which is likely due to formation of G-tetrads or other substructures. Use of high urea concentrations (7.0 M) in the CE buffer did not result in a single-peak analysis either. These problems were not apparent in the analysis of mixed-sequence oligonucleotides and we are investigating the possible

(51) Maureen Cronin, personal communication.

**Scheme 1.** Functionalization of Aminosilated Surfaces for Hybridization and CE Studies

<sup>a</sup> DMT-HEG-CED, 5-ethylthiotetrazole, ACN. <sup>b</sup> I2, THF/H<sub>2</sub>O/pyridine. <sup>c</sup> Piperidine/DMF. <sup>d</sup> Fmoc-HoSer(Trt)-OH, HATU, DIEA, DMF. <sup>e</sup> Ac<sub>2</sub>O, pyridine. <sup>f</sup> TCA, DCM. <sup>g</sup> CPR-I, 5-ethylthiotetrazole, ACN.

reasons for the inability to analyze a polyG prepared on these arrays. Finally, a dT 60mer was synthesized on an array, cleaved, and analyzed by CE. The average step yield for the 60mer, based on the failure pattern, was 98.5%. In addition to the ongoing characterization of the hybridization properties of these arrays, a genotyping assay for analyzing mutations found in three cardiac K-channels associated with long QT syndrome was developed. The results of this study will be published elsewhere.<sup>49</sup>

**Conclusion**

The work described represents a robust and highly flexible method for producing custom oligonucleotide arrays. The process for generating the patterned substrates is very reproducible and the use of surface tension allows for uniform, addressable features. The quality of the oligonucleotides synthesized on these arrays is comparable to that obtained by conventional oligonucleotide synthesis on controlled-pore glass. There is a high percentage of full-length probes in each array feature and the process supports synthesis of oligonucleotides up to 60mers. These arrays have performed well in a variety of hybridization studies. Drop-on-demand piezoelectric nozzle (ink-jet) synthesis makes the arrays readily customizable. Sequentially iterative chip designs require no incremental expense or setup time. The results of using these arrays for genotyping and expression analysis will be reported elsewhere.

**Experimental Section**

**General Materials and Methods.** Unless otherwise noted, all materials were obtained from commercial suppliers and used as received. Adiponitrile was placed over activated 4 Å molecular sieves and stored under argon for at least 14 days prior to use. Milli-Q water refers to water that has been purified to a conductance level of 17.8–18.2 MΩ with particulate matter of greater than 0.2 μm filtered from the water. Glass substrates were obtained from Erie Scientific. Plasma treatments were performed using a Tegal Plasmaline-421 RF oxygen plasma generator according to the manufacturers specifications for the indicated period of time. Spin coating of substrates with Microposit 1818 from Shipley was done on a Laurell Technologies WS-400A-6NPP-Lite spin coater. Chromium-on-quartz masks from Image Technology were used for contact patterning. A custom-manufactured 500 W collimated mercury lamp source (365 nm) operating at 15 mW/cm<sup>2</sup> from AB-M, Inc. was used as the exposure device. Microposit 351 developer from Shipley was used according to the manufacturers specifications. Contact angles were determined using 18 MΩ water and a Tantec Cam-Plus contact angle meter. At least three areas/substrate were assayed and the averages of those measurements are reported. XPS analysis was performed on a Physical Electronics

Quantum 2000 instrument using a monochromated Al Kα X-ray source at 1486.6 eV. The takeoff angle was 45° with an acceptance angle of ±23°. The analysis area was 1.4 mm × 0.5 mm. The data are quantified by using relative sensitivity factors and a model that assumes a homogeneous layer. The analysis depth is considered to be 3 escape depths, from where 95% of the detected photoelectron signal is generated. Escape depths are on the order of 15–35 Å, which leads to an analysis depth of ~50–100 Å. All TOF-SIMS data were generated with a PHI TRIFT II instrument with a Ga<sup>69</sup> liquid metal ion gun primary ion source [12 kV (+)ions, 18 kV (–)ions]. The instrument was operated in an ion microprobe mode so that the bunched, pulsed primary ion beam was rastered across the glass surface. To compensate for charging of the sample, a low-energy electron flood gun was used. Both positive and negative spectra were obtained from each sample and two to three spots on each sample were analyzed.

The drop-on-demand oligonucleotide synthesis was performed on the custom-made Protogene IGOR 50 DNA synthesizer, a fully automated system that uses piezoelectric ink jet technology to print custom DNA chips. The IGOR 50 consists of a Windows PC, a Compumotor 6K4 four axis motor controller, three linear stages for X, Y, and Z motion, a rotational alignment motor, a Matrox vision system, five SMC LVC 200 Teflon valves, and four MicroFab piezoelectric nozzles. All the stages, valves, and nozzles are mounted in a tabletop aluminum structure that provides a dry, nitrogen-filled environment for the synthesis, scans the chip under the nozzles for the nucleoside amidite monomer delivery, and performs all ancillary reagent additions/washes. All machine operations are fully automated under the control of the Windows PC with the real time control done by the Compumotor 6K4 controller. Operators use a Matrox vision system to align the nozzles to the synthesis features patterned on the chips as part of the system setup. The firing of the piezoelectric nozzles is controlled by a single board computer from Real Time Devices with 4 analogue outputs, one per nucleoside amidite that generates a bipolar square wave at 5 kHz, which ejects approximately 200 pL of amidite solution per pulse. The sequence file is downloaded from the PC to the single board computer, which synchronizes in hardware the movement of the chip under the nozzles and dispenses the solutions onto the hydrophilic synthesis features of the prepared surface tension chips. Capillary electrophoresis was carried out on a Beckman P/ACE 5000 system. Samples were injected electrokinetically onto a 37 cm × 75 μm i.d. J&W Scientific 3% T 3% C μPAGE polyacrylamide gel filled column. Separation was done at 9 kV and the separation buffer used was Tris-borate at pH 8.0 with 7 M urea. After separation, peaks were integrated by using the Beckman P/ACE Station software and peak height and area were used to determine stepwise coupling yields by comparison of the full length product to the failure sequences with the differences in extinction coefficient taken into account for each peak. The average of the results from the area and height calculations was used in the determination of the coupling yields.

**Substrate Washing.** Glass substrates were cleaned by sonication in a 5% solution of Cole-Parmer Micro 90 in Milli-Q water for 60 min



at room temperature. The substrates were then rinsed exhaustively with Milli-Q water and dried with filtered nitrogen. The substrates were then exposed to an RF oxygen plasma (0.05 Torr, flow rate of 3.5 mL/min, 150 W) for 30 min and further washed for 10 min in a Piranha solution. **PIRANHA WARNING. CAUTION:** Piranha solution is composed of 70% concentrated sulfuric acid and 30% hydrogen peroxide. This solution reacts violently with organic solvents and is a severe skin irritant. Extreme caution should be exercised when handling this solution. The substrates were rinsed again with Milli-Q water, dried under a stream of nitrogen, and subjected to a second oxygen plasma treatment.

**Surface Tension Array Preparation.** Immediately following cleaning, the substrates were silylated with a 0.4% solution of **1** in anhydrous toluene under argon for 72 h. The substrates were then washed in anhydrous toluene with sonication for 15 min and then washed in 95% ethanol with sonication for 15 min. After drying each substrate under argon, they were cured either for 30 min at 120 °C or in vacuo at 55 °C for 18 h. Next, each substrate was coated with 3.4 mL of photoresist and spun at 1250 rpm for 30 s to give a final thickness of 2.3–2.5  $\mu\text{m}$ . After spin coating, the photoresist was soft baked for 30 min at 90 °C. Next, the substrates were patterned by placing each substrate with the photoresist side down onto a chromium-on-quartz mask that had a 19  $\times$  19 array of round features with each feature being 1.0 mm in diameter with center-to-center spacing of 2.0 mm (for the cleavage and CE studies) or a 31  $\times$  81 (250  $\mu\text{m}$  diameter, 508  $\mu\text{m}$  spacing) array for the hybridization work. The substrates were then exposed to near-UV for 1.0 s. After irradiation, the exposed photoresist was removed by placing the substrates into a solution of Microposit 351 developer (1:1 in water) for 30 s with agitation and then rinsed extensively with Milli-Q water and dried under argon. The substrates were then exposed to an RF oxygen plasma for 15 min to remove the adventitious APDMS along with residual photoresist from the photolyzed regions. Next, the substrates were placed in an argon-filled glovebag and treated with a 0.25% solution of **2** in anhydrous toluene for 10 min at room temperature. Following this, the substrates were washed in anhydrous toluene with sonication for 15 min. The photoresist covering the synthesis regions was removed by sonication in acetone. The substrates were then washed in 1-methyl-2-pyrrolidinone (NMP) for 60 min at 70 °C and washed extensively in Milli-Q water and dried under argon.

**Aminosilanation Study.** Seven 1 in.  $\times$  2 in. pieces of glass were cleaned as described (vide supra) and then subjected to treatment with a solution of APDMS in toluene for various times. Thus, a 0.4% solution of APDMS in anhydrous toluene was prepared in a glovebag under an argon atmosphere. The substrates were immersed in this solution for the indicated times. Upon removal from the solution, the substrates were rinsed with a copious amount of toluene followed by a wash with 50% aqueous ethanol. The substrates were then dried under a stream of argon and placed in a separate section of the glovebag until they could be cured. Once all substrates had been treated, they were then subjected to curing at 120 °C for 60 min. At this time, the substrates were removed from the oven and allowed to cool in a desiccated argon atmosphere until they were analyzed.

**Linker Derivatization.** All derivatizations were performed in a chip reaction chamber. Briefly, two arrays were placed with their patterned surfaces facing one another. Four steel binder clips secured a 0.312-in. thick silicone rubber (grade 40A or 50A) gasket between the arrays, and reagents were introduced via syringe through a 27-gauge needle. The gas interior was displaced through an open needle while reagent was being injected with a syringe. At the end of the reaction, the reagent was removed via syringe. For this process, all washings between steps were done by first disassembling the reaction chamber and then rinsing each array individually with the given solvent. Excess solvent was removed from the surface by means of an argon gas stream. A fresh gasket was used for each subsequent chamber assembly and derivatization process.

For arrays used in hybridization studies, prior to in situ synthesis,  $\alpha$ -O-DMT-hexaethylene-glycol- $\omega$ -O-CED phosphoramidite (DMT-HEG-CEP) linker was coupled to the surface-bound amines by using a 1:1 solution of 0.1 M DMT-HEG-CEP and 0.45 M 5-ethylthiotetrazole in acetonitrile for 15 min with mixing (Scheme 1). After two acetonitrile washes the chips were treated with a 0.1 M solution of iodine in

tetrahydrofuran (THF)/pyridine/water for 1 min and then washed twice with acetonitrile. Any uncoupled amines were acylated by treatment with a 25% v/v solution of acetic anhydride in pyridine for 15 min. The arrays were stored in a desiccator until use.

For arrays used in cleavage and CE analysis studies, the aminoalkylated patterned slides were initially treated with a 20% v/v solution of piperidine in anhydrous dimethylformamide (DMF) at room temperature for 30 min and then were washed in anhydrous DMF. Next, the arrays were assembled into a reaction chamber and a 0.1 M solution of *N*- $\alpha$ -(9-fluorenylmethoxycarbonyl)-*O*-trityl-L-homoserine (Fmoc-HoSer(Trt)-OH) in anhydrous DMF containing 0.1 M *N*-[(dimethylamino)-1*H*-1,2,3-triazol[4,5-*b*]pyridin-1-ylmethylene]-*N*-methylmethanaminium hexafluorophosphate *N*-oxide (HATU) and 0.2 M anhydrous diisopropylethylamine (DIEA) was introduced and allowed to react for 30 min at room temperature. After reagent removal and disassembly, the arrays were washed with DMF. The arrays were treated with a 20% v/v solution of piperidine in anhydrous DMF for 15 min to remove the Fmoc group. The arrays were washed in anhydrous DMF and then treated with a 25% v/v solution of acetic anhydride in pyridine for 30 min to acylate the amine of the homoserine moiety as well as any unreacted surface amines. The arrays were then treated with a 3% v/v solution of trichloroacetic acid (TCA) in dichloromethane (DCM) for 10 min to remove the trityl group. Finally, the arrays were treated with a 1:1 mixture of a 0.1 M solution of CPR-I and 0.45 M 5-ethylthiotetrazole in anhydrous acetonitrile for 5 min. This is shown in Scheme 1. After two washes with anhydrous acetonitrile, the arrays were treated with oxidizing reagent and any unreacted hydroxyl groups were acylated as above. The arrays were stored in a desiccator until use.

**Synthesis.** Drop-on-demand oligonucleotide synthesis was performed on the Protogene IGOR 50 synthesizer using the following reagents and concentrations. The phosphoramidites used were Pac-dA-CE phosphoramidite, Ac-dC-CE phosphoramidite, <sup>3</sup>Pr-Pac-dG-CE phosphoramidite, and dT-CE phosphoramidite (0.1 M). 5-Ethylthiotetrazole (0.45 M) was used as the activator. Amidites and activator were premixed as 1:1 v/v solutions in 10% anhydrous acetonitrile in adiponitrile immediately prior to synthesis. The ancillary reagents consisted of an oxidizer (0.1 M iodine in THF/pyridine/water), Cap mix A (THF/2,6-lutidine/acetic anhydride), Cap mix B (10% 1-methylimidazole/THF), and 3% TCA in DCM. Parallel synthesis of individual oligonucleotides was achieved by addition of individual amidites to the hydrophilic regions of prepared surface tension arrays via piezoelectric ink-jet devices. After coupling for 2 min, unreacted amidite solution was washed off of the surface by flooding with acetonitrile followed by spinning the chip at 2000 rpm for several seconds. The ancillary reagents were added to the surface by flooding the substrate and removed by spinning after suitable reaction times. The synthesis was performed in a closed, argon-saturated environment with a unidirectional flow of the protecting gas.

**Cleavage and Deprotection.** For arrays that were synthesized for hybridization studies, side chain protecting groups were removed by immersion of the array in a 50% v/v solution of ethylenediamine (EDA) in 95% ethanol for 2 h at room temperature with agitation. The substrates were then washed with 95% ethanol and stored in a desiccator until use. For cleavage of oligonucleotides from the surface for CE analysis, substrates were placed in a reaction chamber as described and then treated with 1.0 mL of concentrated ammonium hydroxide for 20 min at room temperature with mixing. The solution was removed from the chamber and side chain deprotection was accomplished by warming the solution to 70 °C for 15 h. After deprotection, the solvent was evaporated in vacuo and the residue was reconstituted in an appropriate amount of Milli-Q water.

**Acknowledgment.** We would like to thank Dr. Greg Strossman and Dr. Patrick H. Schnabel of Charles Evans & Associates (Sunnyvale, CA) for performing the XPS and TOF-SIMS experiments, Dr. Douglas Greiner for his guidance and his critical evaluation of this work, and Dr. Brian Qian and Dr. Roy Tan of Genepharma Inc (Sunnyvale, CA) for their assistance in the preparation of the manuscript. The majority of the research for this manuscript was done at Protogene Labs (Menlo Park, CA).

**Supporting Information Available:** Capillary electropherograms of dT<sub>40</sub>, dT<sub>60</sub>, and dA<sub>40</sub>, determinations and graphical representation of probe consistencies, and a description of the method used to correlate fluorescence signal to hybridizable

probe density (PDF). This material is available free of charge via the Internet at <http://pubs.acs.org>.

JA003758R